

# Interpretation of Sorption Kinetics for Mixtures of Reactive Dyes on Wool

Elif ŞAHİN

*University of Dicle, Faculty of Science and Letters, Department of Chemistry  
21280, Diyarbakır-TURKEY  
e-mail: esahin@dicle.edu.tr*

Received 24.01.2005

The equilibrium sorption isotherms of 3 reactive dyes (C. I. Reactive Yellow 84, C. I. Reactive Red 141, C. I. Reactive Blue 160) and their binary mixtures adsorbed on prewetted wool fiber were investigated. The kinetic studies were carried out at  $\text{pH} \leq 7$  and  $80^\circ\text{C}$  in dye solutions containing 20 g/L NaCl. It was reported that binary mixtures of these reactive dyes have lower sorption values than the dyes alone, at the same dye concentration, pH and temperature. The isotherms obtained are Langmuir type. The rate parameters of adsorption kinetics decrease with increasing dye concentration.

**Key Words:** Dye adsorption, Kinetic model, Reactive dye.

## Introduction

The effects of pH, electrolyte concentration and temperature on the fixation of reactive dyes on cotton fiber have been studied for over 50 years<sup>1-5</sup>. Reactive dyes are one of the most popular classes of dye-stuffs. They can fix to fabric by the formation of a covalent bond, which is an advantage over other classes of dyes, since such reactive dyes can be immobilized via physical adsorption or mechanical entrapment<sup>1</sup>. Control of dye sorption kinetics is very important, since the final shade depends strongly on the dye concentration in the fiber at the end of the dyeing process, and equilibrium is unlikely to be reached in practice. A dye-dye interaction involving dye molecules of the same structure is called aggregation<sup>3</sup>. The extent of dye aggregation decreases with increasing temperature<sup>4</sup>. Aggregation increases with increases in dye concentration and in ionic strength<sup>5</sup>. Many researchers have made quantitative measurements of aggregation of single dyes in aqueous solutions<sup>(6,7)</sup>, but none have quantified a correlation between aggregation in solution and dyeing kinetics. Furthermore, several authors have developed mathematical techniques to predict the equilibrium exhaustion of dyes applied in mixtures when no interaction occurs in solution<sup>(8,9)</sup>. Compton concluded that dye fixation to the fabric is controlled by a solid-liquid interfacial process that is first order with respect to the surface concentration of the dye<sup>10</sup>. Disaggregants and dispersants affect the rate of dye uptake by decreasing the degree of aggregation of dyes in solution<sup>11</sup>. Matyjas et al. used Vickerstaff's model for examining the kinetics of reactive dyes, and determined the effect of dye structure on adsorption<sup>12</sup>.

Although many articles on dyeing processes have been published, there are only a few papers on kinetic investigations<sup>13</sup>. Kim and Lewis examined the effect of various anti-setting systems and reactive dyeing systems for wool fibers<sup>14</sup>. Cho and Lewis investigated the dyeing properties of hetero-bifunctional reactive dyes during the dyeing cycle and the application of specially prepared hetero-bifunctional and related model dyes on wool<sup>(15,16)</sup>. The Procion HE dye used had a relatively large molecular size, which could make it difficult to penetrate and diffuse within the wool fiber, producing more ring dyeings<sup>(15,17)</sup>.

This study focused on the adsorption and sorption rate constants of reactive dyes and dye mixtures on wool. The Langmuir kinetic model was used in determining adsorption and desorption rate constants for the dyes *C. I. Reactive Yellow 84*, *C. I. Reactive Red 141* and *C. I. Reactive Blue 160*.

## Experimental

### Materials

Woven wool serge fiber (semi-decated, scoured and dried, New Zealand code number PS 10Z8048) supplied by a textile dyeing facility in Kayseri, Turkey, was used. The reactive dyes [Procion Yellow HE4R (*CI Reactive Yellow 84*), Procion Red HE7B (*CI Reactive Red 141*), Procion Blue HERD (*CI Reactive Blue 160*)] were obtained from Ciba and used without any further purification. An NEL-pH 890 pH-meter and buffer solutions (0.05 M NaHCO<sub>3</sub> and 0.1 M NaOH) were used to adjust pH values. The absorbance values of the dyebath at each stage were measured using a UV/Vis spectrophotometer (Shimadzu UV-160). All dyeings were carried out in a reactor system under the following conditions: pH: 7; temperature: 80 °C; electrolyte concentrations: 20 g/L NaCl; dye concentrations: 0.07, 0.13, 0.25, 0.50, 0.75, 1.00, 1.25 and 1.50 g/L for single and binary dyeing; dyebath volume: 100 mL; time of dyeing: 2 h for single and 3 h for mixtures (or until equilibrium is reached); wool fiber: 0.5 g; liquor ratio: 200:1. Dye concentrations were determined for single and binary dyeing using spectrophotometry data at the  $\lambda_{max}$  of each dye.

### Designations

$C_s$  - equilibrium concentration of dye in dyebath [g/100 mL],

$C_f$  - dye concentration in fiber [g/100 g fiber],

$S$  - dyeing capacity of the fiber or adsorption capacity of the adsorbent [g /100 g fiber],

$K_L$  - adsorptivity capacity at low dye concentrations of adsorbate or adsorptivity capacity at low concentrations of adsorbate [100 mL/g],

$a$  - absorptivity [L/g cm],

$t$  - time of dyeing [min],

$k_a$  - adsorption rate constant [100 mL/g min],

$k_d$  - desorption rate constant [min<sup>-1</sup>],

$R^2$  - linear correlation coefficient

Y - Procion Yellow HE4R (*CI Reactive Yellow 84*),

R - Procion Red HE7B (*CI Reactive Red 141*),

B - Procion Blue HERD (*CI Reactive Blue 160*)

YR - Y is in Y with R binary dyes

YB - Y is in Y with B binary dyes  
 RY - R is in R with Y binary dyes  
 RB - R is in R with B binary dyes  
 BR - B is in B with R binary dyes  
 BY - B is in B with Y binary dyes

## Spectroscopic characterization

### Single dyes

The maximum absorbance wavelengths for the 3 direct dyes were used to determine  $C_s$  values. Known amounts of samples with appropriate dilution were taken from the dyebath after the dyeing procedure. Calibration curves were used for this determination.

### Binary dyes

Due to the interaction between the 3 reactive dyes, equilibrium dye concentrations  $C_s$  were determined according to the method below<sup>13</sup>.

In the case of  $\lambda_1 < \lambda_2$ , absorption measurements were obtained at these wavelengths.

$$At\lambda_1 \quad A_1 = a_{\lambda_1,B} \cdot C_B + a_{\lambda_1,R} \cdot C_R \quad (1)$$

$$At\lambda_2 \quad A_2 = a'_{\lambda_2,B} \cdot C_B + a'_{\lambda_2,R} \cdot C_R \quad (2)$$

where B denotes the blue dye, R represents the red dye, and  $\lambda_1$  and  $\lambda_2$  stand for the maximum absorbance wavelengths for the blue and red dyes, respectively. In order to determine  $C_B$  and  $C_R$  values from these 2 equations,  $a_{\lambda_1,B}$ ,  $a_{\lambda_1,R}$ ,  $a'_{\lambda_2,B}$  and  $a'_{\lambda_2,R}$  should be known. Absorption for pure B and R compounds at certain  $C_B$  and  $C_R$  concentrations are measured at  $\lambda_1$  and  $\lambda_2$ .

$$A_1 = a_{\lambda_1,B} \cdot C_B \quad A_1 = a_{\lambda_1,R} \cdot C_R$$

$$A_2 = a'_{\lambda_2,B} \cdot C_B \quad A_2 = a'_{\lambda_2,R} \cdot C_R$$

$a_{\lambda_1,B}$ ,  $a_{\lambda_1,R}$ ,  $a'_{\lambda_2,B}$  and  $a'_{\lambda_2,R}$  values are calculated. By using equations (1) and (2)  $C_B$  and  $C_R$  values are determined. This method can be applied to  $n$  components in solution by measurements at  $n$  different wavelengths.

## Adsorption dye characterization

The results of dyeing measurements may be reported as sorption isotherms, i.e. the variation in the ratio of the equilibrium dye concentration on fiber to that of the dyebath at constant temperature<sup>6</sup>. In order to understand the trend of the sorption isotherms, a logarithmic regression curve was fitted to the scatter plot of equilibrium concentrations of dye in the fiber and in the dyebath. All the logarithmic regression isotherm curves exhibit an initial smooth rising pattern, followed by a flat plateau where the sorption remains practically constant over a wide range of dyebath concentrations. Regression analysis of sorption isotherms with the standard known isotherms of Nernst, Freundlich and Langmuir shows that the Langmuir is the best to correlate sorption data for both single dyes and dye mixtures. Regression analysis was used to determine the best model for understanding the dyeing sorption isotherms of the 3 dyes under consideration and their binary mixtures.

The Freundlich sorption isotherm equation is given by

$$C_f = S \cdot (C_s)^{1/K_L}$$

When solved linearly the following equation is obtained:

$$\log C_f = \log S + K_L \cdot \log C_s$$

The Langmuir sorption isotherm equation is written as

$$C_f = \frac{S \cdot K_L \cdot C_s}{1 + K_L \cdot C_s}$$

and its linear equation is given by

$$\frac{C_f}{C_s} = K_L \cdot S - K_L \cdot C_f$$

### Kinetic dye characterization

The equation for overall dyeing rate that idealized the Langmuir kinetic model<sup>13</sup>

$$\nu = \frac{\partial C_f}{\partial t} = k_a \cdot (C_s) \cdot (S - C_f) - k_d \cdot (C_f)$$

was used in the determination of dye concentrations at given time intervals, and dyeing rate constants were determined using this model. When equilibrium is reached,  $\partial C_f / \partial t = 0$  indicates a kinetic balance between opposing rates of adsorption and desorption of dye.

#### *Determining S and K<sub>L</sub>*

For the Langmuir kinetic model the parameters  $S$  and  $K_L$  were calculated using the  $C_s$  and  $C_f$ :

$$K_L = \frac{k_a}{k_d} = \frac{C_f^\infty}{C_s^\infty \cdot (S - C_f^\infty)}$$

In the plot of  $C_f^\infty / C_s^\infty$  versus  $C_f^\infty$  (commonly known as a Scatchard plot), the slope is  $-K_L$  and the intercept is  $K_L \cdot S$ .

#### *Determining adsorption rate constants, k<sub>a</sub>*

The adsorption rate constant,  $k_a$ , was calculated using a short-time approximation of the Langmuir kinetic model. In the early dyeing process ( $t \rightarrow 0$ ),  $C_f$  is near zero and  $(S - C_f) \approx S$ ; hence the equation becomes

$$\frac{\partial C_f}{\partial t} = k_a \cdot C_s \cdot S$$

Rearranging to solve for  $k_a$  yields

$$k_a = \lim_{t \rightarrow 0} \left[ \left( \frac{\partial C_f}{\partial t} \right) / C_s \cdot S \right]$$

*Determining desorption rate constants,  $k_d$* 

The desorption rate constant was also determined using a short-time approximation of the Langmuir kinetic model. Early in the washing process ( $t \rightarrow 0$ )  $C_s$  is near zero; hence the equation becomes

$$k_d = \lim_{t \rightarrow 0} \left[ - \left( \frac{\partial C_f}{\partial t} \right) / C_f \right]$$

## Results and Discussion

The maximum wavelengths of the 3 reactive dyes used in this study were as follows (nm): 410, 544 and 617 for *CI Reactive Yellow 84*, *CI Reactive Red 141*, and *CI Reactive Blue 160*, respectively. Dyeing was applied and experimental data for the isotherms were obtained. To understand the trend of the sorption isotherms, a logarithmic regression curve was fitted to the plot of equilibrium concentrations of dye in the fiber and in the dyebath and the results are shown in Figure 1. The high values of  $R^2$  along with the smooth distribution of points demonstrate that the isotherms characterized by single and binary mixtures of Y, R and B are more suitable for linear Langmuir isotherms (Figure 2).

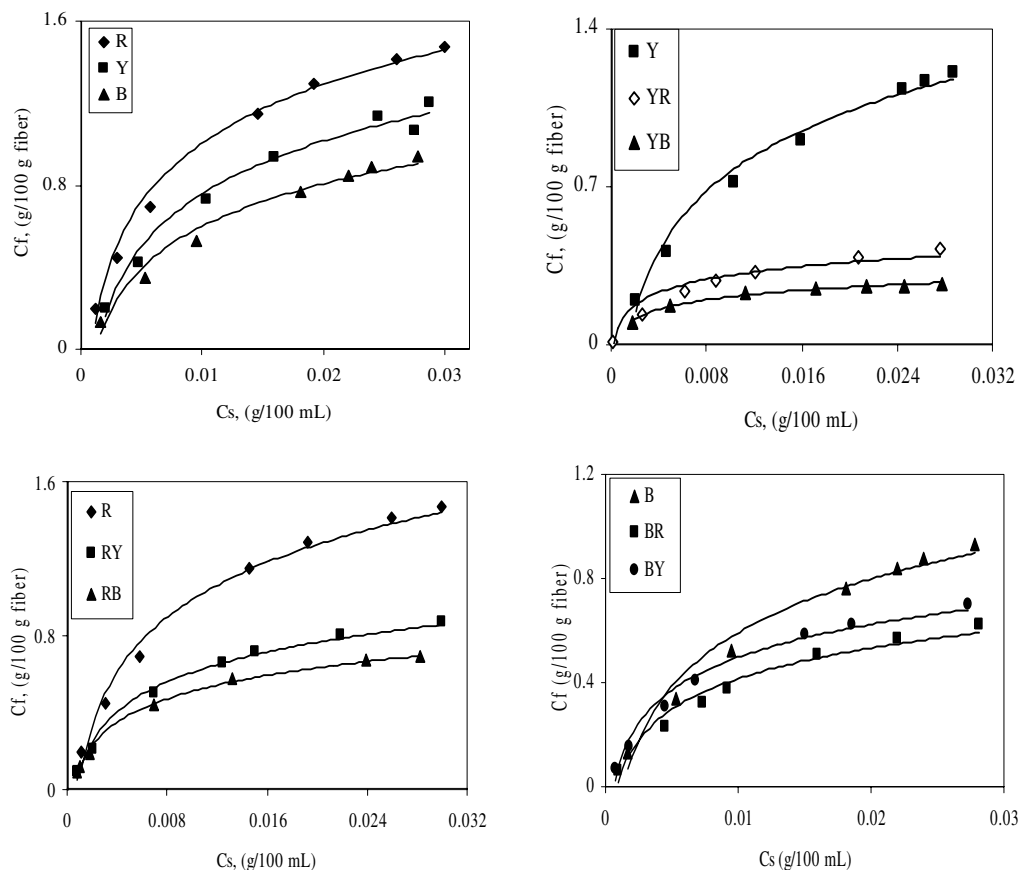


**Figure 1.** Adsorption isotherms of Y, R, B in single and binary mixtures at 80 °C.

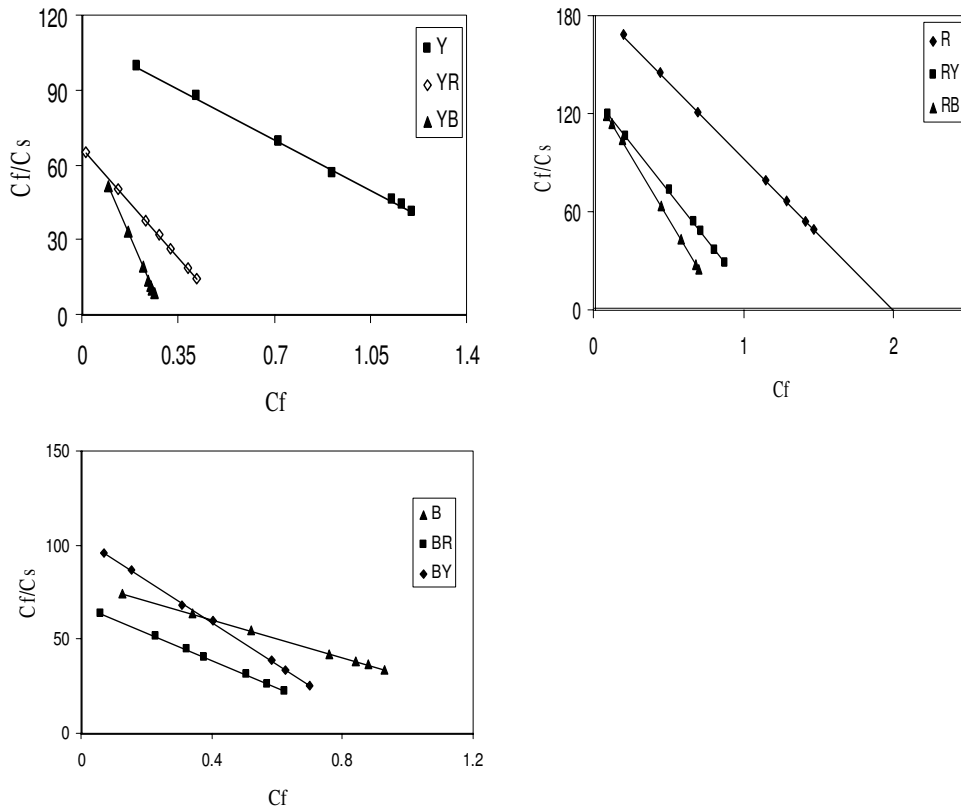


**Figure 2.** Linear Langmuir adsorption isotherms of Y, R and B in single and binary mixtures at 80 oC. Y ( $R^2 = 0.9989$ ); YR ( $R^2 = 0.9999$ ); YB ( $R^2 = 0.9993$ ); R ( $R^2 = 0.9999$ ); RY ( $R^2 = 0.9999$ ); RB ( $R^2 = 0.9999$ ); B ( $R^2 = 0.9995$ ); BR ( $R^2 = 0.9994$ ); BY ( $R^2 = 0.9998$ ).

*Single dyeing*

The R dye was better adsorbed than the Y and B dyes, as shown in Figure 1. The R dye has a better adsorbing capacity at low and higher concentrations compared to the Y and B dyes. Values of  $S$  and  $K_L$  for these dyes are given in Table 1. The values of  $S$  for each of the 3 single dyes are very consistent, with a mean value of 1.9 g/100 g fiber. If the  $S$  values for a set of dyes varied widely, the predicted total dye concentration in the fiber under equilibrium conditions would vary widely between the dyes. The  $K_L$  values correspond to the dyeing rates:  $K_L = k_a / k_d$ . From the  $K_L$  values determined, the apparent affinities of these dyes rank as follows:  $R > Y > B$ .

*Binary dyeing*

Figure 1 shows that the Y dye has a better adsorbing capacity compared to the R and B dyes. The values obtained from the binary mixtures fit the Langmuir isotherm type. The  $K_L$  constants in this dyeing are YB ( $K_L = 253.3$ ) > RB ( $K_L = 154.8$ ) > YR ( $K_L = 124.5$ ) > RY ( $K_L = 116.9$ ) > BY ( $K_L = 111.8$ ) > BR ( $K_L = 73.5$ ).

**Table 1.** Estimated  $S$  [g/100 g fiber] and  $K_L$ [100 mL/g] values.

	$S$	$K_L$
Y	1.9	58.1
YR	1.9	124.5
YB	3.3	253.3
R	2.0	93.2
RY	1.1	116.9
RB	1.2	154.8
B	1.7	81.2
BR	0.9	73.5
BY	0.9	111.8

In order to form the short-time approximation of the Langmuir kinetic model, only data between 0 to 60 min were used to determine initial dye adsorption rate constants. As seen in Figure 3, the first data point of each dye deviates from their linear curves since the wool fiber was pre-wetted prior to dyeing. When the pre-wetted wool fiber was placed in a dye bath, decreases in concentrations occur due to the dilution of dye on the surface of the fiber. For this reason the first data point was omitted from the least squares model.

Figure 4 shows that adsorption rate constants of dye mixtures decreased more substantially than the adsorption rate constant of single dyes. As the concentrations of dyes increase, the  $k_a$  of dyes decreases drastically.

It is apparent that the value of  $k_a$  decreases as dye concentration increases (Table 2). Aggregation increases with particle size and therefore decreases the rate of diffusion.

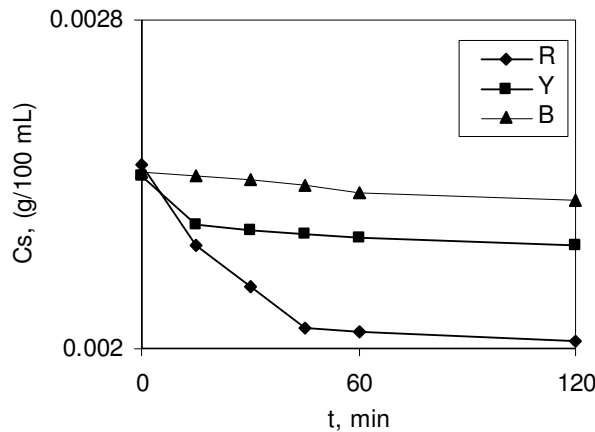


**Figure 3.**  $k_a$  determination of Y, R, B of single dyes.

**Table 2.** Adsorption rate constants ( $k_a$ ) of single dyes [100 mL/g min].

Conc., g/L	Y	R	B
0.13	0.780	0.873	0.999
0.25	0.760	0.867	0.992
0.50	0.750	0.865	0.990
0.75	0.740	0.862	0.985
1.00	0.730	0.860	0.980
1.25	0.710	0.858	0.978
1.50	0.700	0.855	0.976

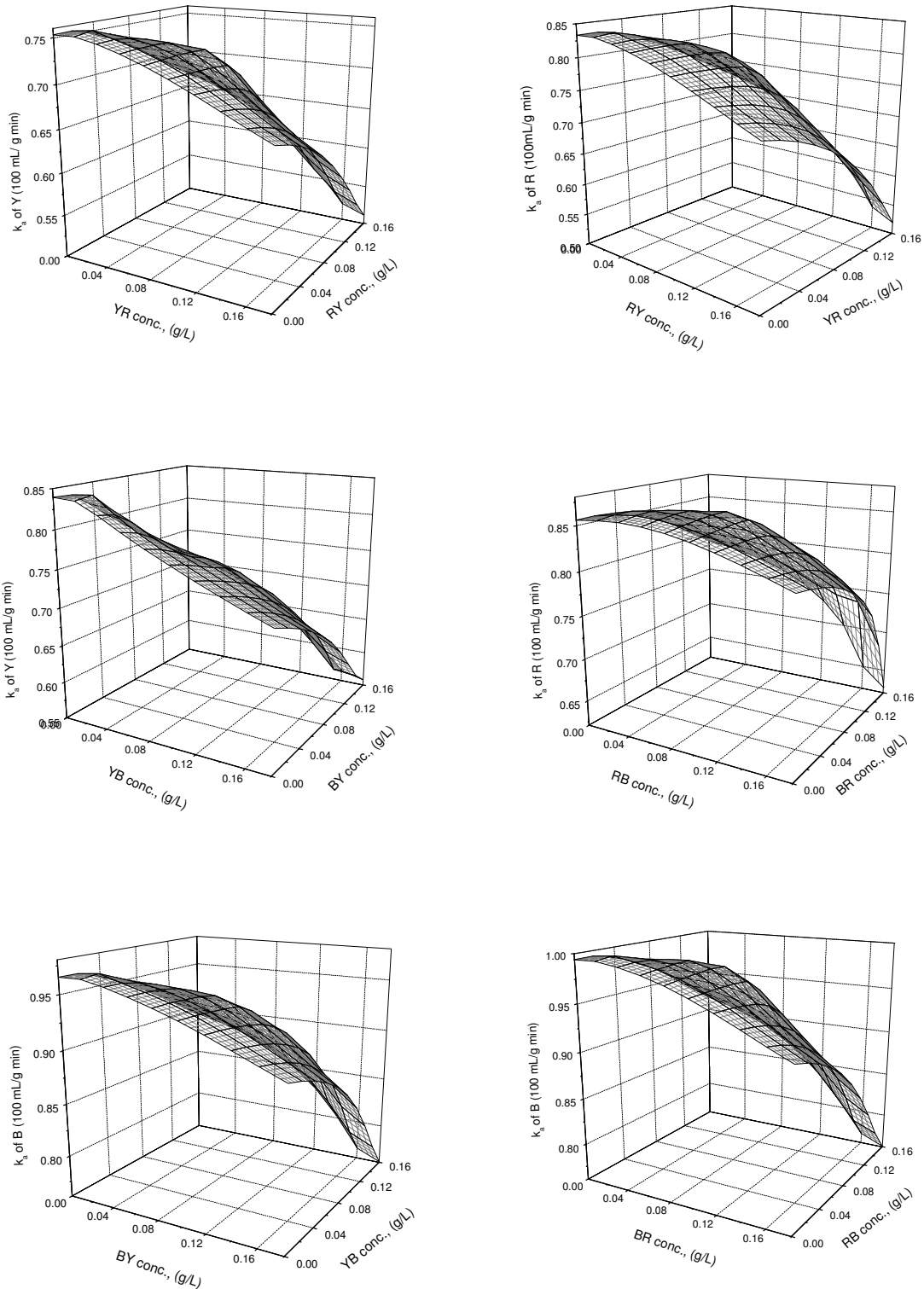


**Figure 4.** Adsorption rate constants ( $k_a$ ) of binary dyes [100 mL/g min].

The desorption rate constant values given in Table 3 show that the values of  $k_d$  do not change with dye concentration in solution, hence indicating that dye desorption can be described by a rate constant that does not depend on the solution concentration of dyes.



**Table 3.** Desorption rate constants ( $k_d$ ) of single dyes [ $\text{min}^{-1}$ ].

	Y	R	B
$k_d[\text{min}^{-1}]$	0.012	0.009	0.001

## Conclusions

This investigation looks into the relationship between the kinetic behaviors of reactive dyes. It improves the prediction accuracy of kinetic models in order to estimate the outcome of dyeing and thereby control dye exhaustion to ensure a better shade match. It has been found that the sorption processes in wool fiber proceed in accordance with the model of reaction proposed by Langmuir. The Langmuir kinetic model for dyes Y, R and B in mixtures shows that the aggregation and interaction of dyes in solution is an important factor that causes deviations from adsorption and kinetic behavior. It is apparent that the value of  $k_a$  decreases as dye concentration increases. The desorption rate constant values show that the values of  $k_d$  does not change with dye concentration in solution, hence indicating that dye desorption can be described by a rate constant that does not depend on the solution concentration of dyes.

## References

1. J.I. Kroschwitz and M. Howe-Grant, "Kirk-Othmer Encyclopedia of Chemical Technology", 4<sup>th</sup> ed., Vol. 8, New York, Wiley, 1993.
2. H.J. Zollinger, **J. Soc. Dyers. Colour.** **110**, 209-209 (1994).
3. F. Jones and D.R. Kent, **Dyes Pigments** **1**, 39-48 (1980).
4. M. Greenhalgh, A. Johnson and R.H. Peters, **J. Soc. Dyers. Colour.** **78**, 315-321 (1962).
5. T. Hihara, Y. Okada and Z. Morita, **Dyes Pigments** **45**, 131-143 (2000).
6. A. Bairathi, **Textile Chem. Color.** **25**, 41-46 (1993).
7. J.J. Porter, **Textile Chem. Color.** **25**, 27-37 (1993).
8. S.M. Neale and W.A. Stringfellow, **J. Soc. Dyers. Colour.** **59**, 241-249 (1943).
9. J.J. Porter, **AATCC** 126 (1990).
10. K.Y. Tam, E.R. Smith, J. Booth, R.G. Compton, C.M. Brennan and J.H. Atherton, **J. Colloid Interf. Sci.** **186**, 387-398 (1997).
11. S.Y. Kamat and A.K. Prasad, **Ind. Textile J.** **102**, 98-104 (1991).
12. E. Matyjas, K. Blus and E. Rybicki, **Fibers Text. East. Eur.** **11**, 66-70 (2003).
13. K.R. Beck, T.A. Madderra and C.B. Smith, **Textile Chem. Color.** **23**, 23-27 (1991).
14. J. Kim and D.M. Lewis, **Color. Tech.** **118**, 121-124 (2002).
15. H.J. Cho and D.M. Lewis, **Color. Tech.** **118**, 220-225 (2002).
16. H.J. Cho and D.M. Lewis, **Color. Tech.** **119**, 1-9 (2003).
17. H.J. Cho and D.M. Lewis, **Color. Tech.** **118**, 198-204 (2002).